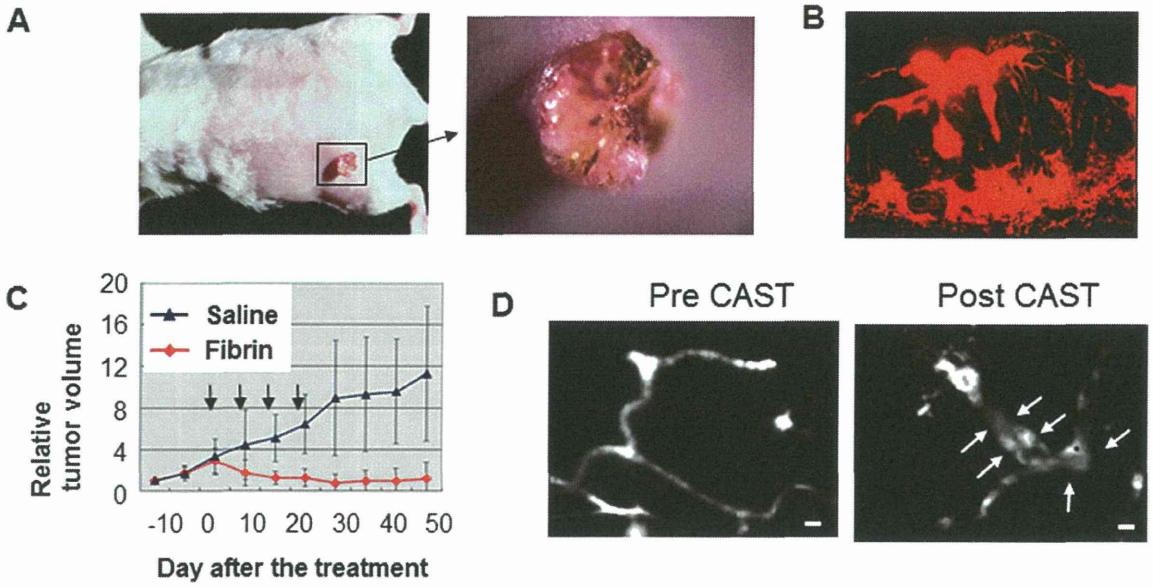

Fig. 6. Anti-fibrin ADC. (A) Chemically induced skin cancer model. (B) Immunostaining of fibrin (red). (C) Anti-tumor effect of anti-fibrin ADC is compared with control (saline). (D) Destroyed tumor vasculature (right column) is shown in comparison with pretreatment (left column). Scale bar, 10 μm.

peared from healing traumatic wound, whereas they still accumulated in the non-healing tumor (Fig. 4).

Anti-tumor activity of CAST therapy

We used a PC xenograft model to examine the anti-tumor effect of anti-collagen ADC compared with anti-CD20 ADC as non-specific targeting, anti-EpCAM ADC as specific cell targeting or saline as a control. Anti-collagen IV ADC exerted the most potent antitumor activity among them[7, 8] (Fig. 5A). Destroyed tumor vasculature that involved empty sleeves of basement membrane was observed[7, 8] (Fig. 5B). There was no hepatotoxicity, nephrotoxicity or bone marrow toxicity in the treated mice. In addition, no autoimmune disease-like adverse effects such as arthritis were observed upon the administration of anti-collagen IV mAb, whereas anti-collagen II mAb combined with lipopolysaccharide caused severe arthritis[7, 8]. There were three issues in the xenograft model: (1) artificial stromal formation (low host reaction because of immunodeficiency, chimera status of mouse & human), (2) no early event of carcinogenesis and (3) rapid growth (leading to overestimation of the drug efficacy because clinical human cancer grows slowly). Therefore, we next used a mouse model of chemically induced skin cancer as a spontaneous tumor for the evaluation of anti-fibrin ADC[6] (Fig. 6A). Anti-fibrin ADC showed strong anti-tumor activity against this fibrin-rich tumor[6] (Fig. 6B and 6C). By in vivo fluorescence endomicroscopy, destroyed tumor vasculature was observed after the treatment[6] (Fig. 6D).

Proof of concept study and future prospects

We are now conducting two proof of concept (POC) studies: 1) The pathophysiological specificity of fibrin deposition in malignant diseases has been demonstrated in the immunohistological examination of various human tissues and animal disease models, and 2) the specificity of anti-fibrin mAb has also been validated in an immunoPET/CT imaging study by a third research group (Hisada *et al.*, unpublished data).

In this review, we have described the tumor stromal barrier and the development of CAST therapy. Besides the stromal barrier, microcirculation, inflammation or blood coagulation affects the pharmacokinetics and efficacy of antibody or ADC in the tumor microenvironment. Among these factors, microcirculation is very important because (1) it is the root between blood vessels and tumor cells (the stromal barrier limit microcirculation), and (2) it regulates tumor growth and metastasis (changes in the microcirculation context have direct effects on the efficacy of the drug). Therefore, we have to understand the mechanism of microcirculation-regulation by further investigation and identify methods of manipulation to develop innovative ADCs including CAST therapy.

Acknowledgments and Funding

Acknowledgements

We thank Dr. T. Sugino, Y. Hisada, Dr. A. Tsuji and Dr. T. Saga for helpful discussions. We also thank Mrs. H. Koike and Mrs. M. Araake-MIzoguchi for technical assistance and Mrs. K. Shiina for secretarial support.

Sources of Funding

This work was supported by the Funding Program for World-Leading Innovative R&D on Science and Technology (FIRST Program) (YM), Third Term Comprehensive Control Research for Cancer from the Ministry of Health, Labour and Welfare of Japan (YM), Grant-in-Aid for Scientific Research on Priority Areas from the Ministry of Education, Culture, Sports, Science and Technology, the Princess Takamatsu Cancer Research Fund (YM), the Japanese Foundation for Multidisciplinary Treatment of Cancer (YM), the National Cancer Center Research and Development Fund (MY), the

Kobayashi Foundation Research Grant for Cancer Research (MY) and Grant-in-Aid for Scientific Research from the Japan Society for the Promotion of Science (MY).

Disclosures
None.

References

1) Imai K, Takaoka A. Comparing antibody and small-molecule therapies for cancer. Nat Rev Cancer. 2006; **6**: 714-727.
2) Wu AM, Senter PD. Arming antibodies: prospects and challenges for immunoconjugates. Nat Biotechnol. 2005; **23**: 1137-1146.
3) Ricart AD, Tolcher AW. Technology insight: cytotoxic drug immunoconjugates for cancer therapy. Nat Clin Pract Oncol. 2007; **4**: 245-255.
4) Dirix LY, Rutten A, Huget P, Dirix M. Trastuzumab emtansine in breast cancer. Expert Opin Biol Ther. 2013; **13**: 607-614.
5) Matsumura Y. Cancer stromal targeting (CAST) therapy. Adv Drug Deliv Rev. 2012; **64**: 710-719.
6) Yasunaga M, Manabe S, Matsumura Y. New concept of cytotoxic immunoconjugate therapy targeting cancer-induced fibrin clots. Cancer Sci. 2011; **102**: 1396-1402.
7) Yasunaga M, Manabe S, Tarin D, Matsumura Y. Cancer stromal targeting therapy by cytotoxic immunoconjugate bound to the collagen IV network in the tumor tissue. Bioconjug Chem. 2011; **22**: 1776-1783.
8) Yasunaga M, Manabe S, Tarin D, Matsumura Y. Tailored immunoconjugate therapy depending on a quantity of tumor stroma. Cancer Sci. 2013; **104**: 231-237.
9) Grapin-Botton A, Melton DA. Endoderm development: from patterning to organogenesis. Trends Genet. 2000; **16**:124-130.
10) Rossi JM, Dunn NR, Hogan BL, Zaret KS. Distinct mesodermal signals, including BMPs from the septum transversum mesenchyme, are required in combination for hepatogenesis from the endoderm. Genes Dev. 2001; **15**: 1998-2009.
11) Yasunaga M, Nisikawa S. Production of endoderm-derived visceral organ cells from ES cells. Tanpakushitsu Kakusan Koso. 2007; **52**: 57-66.
12) Cheng CY, Mruk DD. The blood-testis barrier and its implications for male contraception. Pharmacol Rev. 2012; **64**: 16-64.
13) Dvorak HF, Senger DR, Dvorak AM. Fibrin as a component of the tumor stroma: origins and biological significance. Cancer Metastasis Rev. 1983; **2**: 41-73.
14) Liotta LA, Kohn EC. The microenvironment of the tumour-host interface. Nature. 2001; **411(6835)**: 375-379.
15) Marx J. Cancer biology. All in the stroma: cancer's Cosa Nostra. Science. 2008; **320**: 38-41.
16) Tarin D. Tissue interactions in morphogenesis, morphostasis and carcinogenesis J Theor Biol. 1972; **34**: 6172.
17) Tarin D, Price JE. Influence of microenvironment and vascular anatomy on "metastatic" colonization potential of mammary tumors. Cancer Res 1981; **41**: 36043609.
18) Matsumura Y, Maeda H. A new concept for macromolecular therapeutics in cancer chemotherapy: mechanism of tumoritropic accumulation of proteins and the antitumor agent smancs. Cancer Res. 1986; **46**: 6387-6392.
19) Nakahara T, Norberg SM, Shalinsky DR, Hu-Lowe DD, McDonald DM. Effect of inhibition of vascular endothelial growth factor signaling on distribution of extravasated antibodies in tumors. Cancer Res. 2006; **66**:1434-1445.
20) Lee CM, Tannock IF. The distribution of the therapeutic monoclonal antibodies cetuximab and trastuzumab within solid tumors. BMC Cancer. 2010 **10**:255.
21) Richmond A, Su Y. Mouse xenograft models vs GEM models for human cancer therapeutics. Dis Model Mech. 2008; **2-3**:78-82.
22) Olive KP, Jacobetz MA, Davidson CJ, Gopinathan A, McIntyre D, Honess D, *et al*. Inhibition of Hedgehog signaling enhances delivery of chemotherapy in a mouse model of pancreatic cancer. Science. 2009; **324**:1457-1461.
23) Dimou A, Syrigos KN, Saif MW. Overcoming the stromal barrier: technologies to optimize drug delivery in pancreatic cancer. Ther Adv Med Oncol. 2012; **5**:271-279.

IJC
International Journal of Cancer

Effect of combined treatment with the epirubicin-incorporating micelles (NC-6300) and 1,2-diaminocyclohexane platinum (II)-incorporating micelles (NC-4016) on a human gastric cancer model

Yoshiyuki Yamamoto[1,2], Ichinosuke Hyodo[2], Misato Takigahira[1], Yoshikatsu Koga[1], Masahiro Yasunaga[1], Mitsunori Harada[3], Tatsuyuki Hayashi[3], Yasuki Kato[3] and Yasuhiro Matsumura[1]

[1] Division of Developmental Therapeutics, Research Center for Innovative Oncology, National Cancer Center Hospital East, Kashiwa, Chiba, Japan
[2] Department of Gastroenterology and Hepatology, Institute of Clinical Medicine, Graduate School of Comprehensive Human Sciences, University of Tsukuba, Tsukuba, Ibaraki, Japan
[3] Research Division, NanoCarrier Co., Ltd, Kashiwa, Chiba, Japan

Anticancer agent-incorporating polymeric micelles accumulate effectively in tumors *via* the enhanced permeability and retention effect to exert potent antitumor effects. However, combined use of such micelles has not been elucidated. We compared the effect of combining the epirubicin-incorporating micelle NC-6300 and 1,2-diaminocyclohexane platinum (II) (oxaliplatin parent complex)-incorporating micelle NC-4016 (NCs) with that of epirubicin and oxaliplatin (E/O) in 44As3Luc cells using the combination index method. The *in vivo* antitumor activities of NCs and E/O were evaluated in mice bearing 44As3Luc xenografts. Pharmacokinetic analysis was performed by high-performance liquid chromatography and mass spectrometry. Cardiotoxicity of NC-6300 and epirubicin was assessed by echocardiography. Neurotoxicity of NC-4016 and oxaliplatin was evaluated by examining the paw withdrawal response to noxious mechanical stimuli. NCs showed a highly synergistic activity equivalent to E/O. *In vivo*, NCs exhibited higher antitumor activity in the subcutaneous tumor model and longer overall survival in the orthotopic tumor model than E/O ($p < 0.001$, $p = 0.015$, respectively). The intratumor concentrations of epirubicin and platinum were significantly higher following NCs than following E/O administration. Moreover, the micelles showed lower cardiotoxicity and neurotoxicity than the corresponding conventional drugs. The combined use of the micelles was associated with remarkable efficacy and favorable toxicities in the human gastric cancer model, and warrants the conduct of clinical trials.

The therapeutic window of cytotoxic anticancer agents (ACAs) is known to be narrow; at concentrations falling outside this window, these agents either fail to work or cause severe adverse events. To overcome this drawback, drug delivery systems have been developed. By utilizing the enhanced permeability and retention (EPR) effect, based on the leaky blood vessels and impaired lymphatic drainage in tumor tissues, drug delivery systems in nanoparticle-form enable ACAs to accumulate selectively in the tumors and exert prominent antitumor effect while decreasing the toxicity of the drug payload.[1] Several preclinical studies have demonstrated the advantages of using ACA-incorporating polymeric micelles, and some are currently under clinical evaluation as single micelle agents alone[2–6] or single micelle agents in

Key words: gastric cancer, combination chemotherapy, polymeric micelle, NC-6300, NC-4016

Abbreviations: ACA: anticancer agent; ALT: alanine aminotransferase; AST, aspartate aminotransferase; BUN: blood urea nitrogen; CI: combination index; DACHP: 1,2-diaminocyclohexane platinum (II); DDS: drug delivery system; E/O: epirubicin and oxaliplatin; EF: ejection fraction; EPI: epirubicin; EPR effect: enhanced permeability and retention effect; Fa: the fractional-affected; HPLC: high-performance liquid chromatography; IC50: The 50% inhibitory concentration; ICP-MS: inductively coupled plasma mass spectrometry; NCs: NC-6300 and NC-4016; Pt: platinum; TV: the tumor volume

Grant sponsors: World-Leading Innovative R&D on Science and Technology, National Cancer Center Research and Development Fund, Ministry of Health, Labour and Welfare, Third Term Comprehensive Control Research for Cancer
DOI: 10.1002/ijc.28651
History: Received 16 Aug 2013; Accepted 15 Nov 2013; Online 3 Dec 2013

Correspondence to: Yasuhiro Matsumura, Division of Developmental Therapeutics, Research Center for Innovative Oncology, National Cancer Center Hospital East, 6-5-1 Kashiwanoha, Kashiwa, Chiba 277-8577, Japan, Tel.: +81-(0)-4-7133-1111 (Ex: 5400), Fax: +81-(0)-4-7134-6866, E-mail: yhmatsum@east.ncc.go.jp

What's new?

Combination chemotherapy is sometimes associated with serious adverse effects that lead to treatment cessation. The combined use of anticancer agent-incorporating polymeric micelles–which enable anticancer agents to exert potent antitumor effects while decreasing the toxicity of the drug payload–may overcome this drawback. Reports of combined use of micellar anti-cancer agents are scarce, however. The present study showed that the combination of epirubicin- and DACHP-incorporating polymeric micelles had a stronger antitumor effect and lower toxicity in gastric cancer xenografts than combined epirubicin and oxaliplatin. These results warrant the conduct of clinical trials of combination treatments with anticancer agent-incorporating micelles.

combination with nonmicelle conventional ACAs.[7–9] However, there are scarcely any reports of combined use of micellar ACAs.[10]

Gastric cancer has a poor prognosis, and represents the second leading cause of cancer mortality worldwide.[11] Although the survival times of patients with advanced gastric cancer have improved with advances in chemotherapy, they remain unsatisfactory.[12–15] The chemotherapeutic regimen for gastric cancer usually comprises a combination of two or three ACAs. While the EOX regimen (epirubicin, oxaliplatin and capecitabine) is considered to be one of the standard treatments in Europe,[13] the median overall survival of patients treated with EOX remains unsatisfactory at 11.2 months. When considering the tolerability, it would be difficult to add more cytotoxic agents to improve the therapeutic power of the EOX regimen. With regard to the use of molecular-targeted agents like everolimus and lapatinib, and of biologics such as cetuximab, panitumumab and bevacizumab, no survival benefit of the addition of these agents except for trastuzumab to the standard chemotherapy has been demonstrated in clinical trials for advanced gastric cancer.[16] Under these circumstances, we thought that the idea of replacing two or more of the key cytotoxic agents with their corresponding ACA-incorporating polymeric micelles may be of benefit for cancer patients.

Epirubicin, an anthracycline antitumor drug, has been approved for the treatment of various human cancers.[17,18] However, the anthracyclines have significant dose-limiting cardiotoxicity. Although epirubicin exerts ~33% lower cardiotoxicity than doxorubicin, it remains a serious clinical issue.[19] There are currently no effective therapies to prevent or reduce this cardiotoxicity. Against this background, NC-6300, polymeric micelles incorporating epibubicin was synthesized. NC-6300 comprises epirubicin covalently bound to polyethyleneglycol–poly(aspartiate) block copolymer through an acid–labile hydrazone bond. The conjugate spontaneously forms a micellar structure with a mean diameter of 60–70 nm in aqueous media.[20] *In vitro* findings indicated that it showed pH-dependent epirubicin release, namely, the release of epirubicin from NC-6300 accelerated under increasingly acidic conditions. Therefore the effective release of EPI may be expected within lysosomes of the cancer cells after intracellular trafficking. We have reported from preclinical studies that NC-6300 can reduce the cardiotoxicity of epirubicin and enhance its antitumor activity.[20,21] Oxaliplatin is a third-generation platinum drug that is associated with reduced renal toxicity and ototoxicity, which are typical adverse effects of the former-generation platinum drugs. On the other hand, it can cause troublesome peripheral neurotoxicities such as neuropathic pain and cold sensitivity; it has been reported that this neurotoxicity increases in severity as the cumulative dose of oxaliplatin increases, sometimes necessitating discontinuation of therapy in patients in whom the treatment has otherwise been effective.[22] To overcome this significant drawback of the drug, NC-4016, polymeric micelles incorporating 1,2-diaminocyclohexane platinum (II) (DACHP, the oxaliplatin parent complex) were synthesized. NC-4016 were spontaneously formed from the interaction of the platinum of DACHP and the carboxylic moieties of polyethyleneglycol–poly(glutamate) block copolymer. The mean particle size of NC-4016 is 30–40 nm in diameter. In media containing chloride ions, DACHP is released from the micelles through ligand exchange between the carboxylic groups in poly(glutamate) and the chloride ions. Previous studies have demonstrated the efficacy of NC-4016 against various cancer cell lines.[23,24]

In the present study, we evaluated the efficacy of the combined use of NC-6300 and NC-4016 (NCs) in comparison with that of the combined use of epirubicin and oxaliplatin (E/O) in mice bearing human gastric cancer xenografts.

Material and Methods

Drugs

NC-6300 and NC-4016 were prepared by NanoCarrier Co. (Kashiwa, Japan). Epirubicin was purchased from Pfizer Japan (Tokyo, Japan). Oxaliplatin was purchased from Yakult Honsha Co. (Tokyo, Japan).

Cell cultures

44As3 is a human signet-ring cell gastric cancer cell line that spontaneously metastasizes to the peritoneal cavity and produces large volumes of bloody ascites after orthotopic implantation into the gastric wall.[25,26] A 44As3 cell line stably expressing firefly luciferase (44As3Luc) was established to evaluate tumor progression by *in vivo* imaging.[26] 44As3Luc was kindly provided by Dr. K. Yanagihara (National Cancer

Center Hospital East, Kashiwa, Japan). 44As3Luc cells were maintained in RPMI 1640 medium containing 10% fetal bovine serum (Cell Culture Technologies, Gaggenau-Hoerden, Germany), 100 units/mL penicillin, 100 μg/mL streptomycin and 25 μg/mL amphotericin B (Sigma, St. Louis, MO) in a humidified 5% CO_2 atmosphere at 37°C.

In vitro growth-inhibition assay

The growth-inhibitory effects of NC-6300, NC-4016, epirubicin and oxaliplatin were examined by the tetrazolium salt-based proliferation assay (WST-8 assay; Wako Chemicals, Osaka, Japan). 44As3Luc cells were placed in 96-well plates at 3,000 cells/well in a final volume of 100 μL and incubated for 24 h at 37°C. The medium was then removed, and each drug was added in graded concentrations to the wells and incubated for 72 h at 37°C. After medium removal, WST-8 solution (10 μL) and medium (90 μL) were added to the wells, and the plates were incubated for 1 h at 37°C. The growth-inhibitory effects of each drug were assessed in a 96-well spectrophotometric plate reader (SpectraMax 190, Molecular Devices Corp., CA). The 50% inhibitory concentration (IC_{50}) was determined from the dose–response curves.

Drug interaction analysis

The nature of the interactions between NCs, and between E/O against the 44As3Luc cells was evaluated by the combination index (CI) method of Chou and Talalay.[27] Data were analyzed using the Calcusyn software (Biosoft, NY). NC-6300 and NC-4016 or epirubicin and oxaliplatin were combined at fixed ratios spanning the individual IC_{50} values of each of the agents. The IC_{50} values were determined on the basis of the dose–response curves using the WST assay. For any given drug combination, the CI is known to represent the degrees of synergy, additivity and antagonism. It is expressed in terms of the fractional-affected (*Fa*) value, which represents the percentage of cells killed or inhibited by the drug. *Fa*/CI plots were constructed by computer analysis of the data generated from the median effect analysis.

In vivo subcutaneous models

Female BALB/c nu/nu mice were purchased from Japan SLC (Shizuoka, Japan). They were maintained under specific-pathogen-free conditions under a 12/12-h light/dark cycle and provided free access to sterile food, water and cages. Eight-week-old mice were subcutaneously inoculated with 5×10^5 44As3Luc cells in the flank region. On the day the tumor volume reached 300 mm^3, the mice were randomly divided into seven test groups consisting of five mice each (Day 0). The test drugs were administered intravenously on Days 0, 7 and 14 *via* the lateral tail vein. The single-agent therapy groups received NC-6300 8 mg/kg (on an epirubicin basis) or epirubicin 8 mg/kg, or NC-4016 4 mg/kg (on an oxaliplatin basis) or oxaliplatin 4 mg/kg. The combined therapy groups received a combination of NC-6300 8 mg/kg plus NC-4016 4 mg/kg, or epirubicin 8 mg/kg plus oxaliplatin 4 mg/kg. The normal control group received 5% dextrose solution. The length (*a*) and width (*b*) of the tumor masses were measured twice each week, and the tumor volume (TV) was calculated using the following equation: $TV = (a \times b^2)/2$. For humane reasons, the animals in which the tumor volume exceeded 2,000 mm^3 were sacrificed. All animal procedures were performed in compliance with the Guidelines for the Care and Use of Experimental Animals established by the Committee for Animal Experimentation of the National Cancer Center; these guidelines meet the ethical standards required by law and also comply with the guidelines for the use of experimental animals in Japan.

In vivo orthotopic models

A total of 1×10^6 44As3Luc cells were inoculated into the gastric wall of each 6-week-old female BALB/c nu/nu mouse after laparotomy, as described previously.[25,26,28] Seven days after the inoculation (Day 0), the mice were randomly divided into three groups of eight mice each. Randomization was performed on the basis of the bioluminescence images, and the mean values of count per minute were confirmed to be statically identical among the groups. The drugs of each combination therapy were administered at the same doses/*via* the same route as in the aforementioned study using the subcutaneous tumor models, on Days 0, 7 and 14. Control mice were injected with 5% dextrose solution on the same schedule. *In vivo* photon counting analysis was conducted on a cryogenically cooled IVIS system using the Living Image software (Caliper Life Sciences, MA). *In vivo* bioluminescence imaging was performed twice each week from the day of treatment initiation. The body weight of each mouse was also measured. Mortality was checked daily.

Pharmacokinetic analysis

Eighteen days after the inoculation of the 44As3Luc cells into the gastric wall, a pharmacokinetic study was conducted in the female BALB/c nu/nu nude mice. The animals were injected with a combination of NC-6300 8 mg/kg plus NC-4016 4 mg/kg or epirubicin 8 mg/kg plus oxaliplatin 4 mg/kg intravenously. Under general anesthesia, blood was collected *via* cardiac puncture, and the gastric tumor, liver, spleen, kidneys, heart and small intestine were excised at 0.17, 1, 6, 24, 48, 72 and 168 h, respectively, after the drug administration. Pharmacokinetic analysis was conducted using three mice for each time point.

The epirubicin concentrations derived from NC-6300 and conventional epirubicin in each tissue were measured by high-performance liquid chromatography (HPLC) (RF-20AXS, Shimadzu Corporation, Kyoto, Japan). For the case of NC-6300, the concentrations of both the free epirubicin (*i.e.*, that released *in vivo* from NC-6300) and total epirubicin (*i.e.*, that released from NC-6300 plus the remainder of NC-6300) were determined as described previously.[20]

The platinum concentrations derived from NC-4016 and oxaliplatin in each tissue were determined using inductively

coupled plasma mass spectrometry (ICP-MS) (SPG9000, Seiko Instruments, Tokyo, Japan). Platinum concentration in each tissues was measured at 0.17, 6 and 24 h after the intravenous injection. For the quantitative determination of platinum content, blood samples were centrifuged at 1600 G for 15 min, and then plasma was diluted with 0.1% HNO_3. The other tissue samples were digested with a mixture of 98% H_2SO_4 and 62% HNO_3 (1:2, v:v) and then analyzed by ICP.

Hematotoxicity, hepatotoxicity and nephrotoxicity of the combination therapies

Eight-week-old female CD1 (ICR) mice (Charles River Japan, Kanagawa, Japan) were randomly divided into two groups (Day 0). The drugs of each combination therapy were administered at the same doses/*via* the same route as for the *in vivo* tumor growth inhibition assay, on Days 0, 7 and 14. Blood samples were taken every 7 days from three mice in each group *via* cardiac puncture under general anesthesia. In each blood sample, the white blood cells (WBCs), red blood cells (RBCs) and platelets were counted using Celltac α MEK-6358 (NIHON KODEN, Tokyo, Japan). In addition, the plasma concentrations of aspartate aminotransferase (AST), alanine aminotransferase (ALT), blood urea nitrogen (BUN) and creatinine were measured in SRL Laboratories (Tokyo, Japan).

Cardiotoxicity of NC-6300 versus epirubicin

To compare the cardiotoxicities of NC-6300 and epirubicin, 7-week-old female C57BL/6NCr mice ($n = 7$; Japan SLC, Shizuoka, Japan) were administered NC-6300 8 mg/kg or epirubicin 8 mg/kg on Days 0, 7 and 14 every 4 weeks over a period of 8 weeks (six doses in total). Control mice were injected with 5% dextrose solution on the same schedule. Echocardiography was performed once per week using a high-resolution Micro Ultrasound system (Vevo 770, VisualSonics, Toronto, Canada) equipped with a 40-MHz ultrasound probe (RMV704, VisualSonics). The mice were kept under light sedation with 1–2% isoflurane until the heart rate stabilized from 350 to 450 beats per minute. The left-ventricular dimensions and wall thickness were measured on the parasternal long-axis views, and the ejection fraction (EF) was automatically calculated from the structural parameters using the Vevo 770 software.

Neurotoxicity of NC-4016 versus oxaliplatin

We investigated the neurotoxicities of NC-4016 and oxaliplatin using the nocifensive behavior of paw withdrawal from noxious mechanical stimuli.[29] Six-week-old female DBA/2N mice (Charles River Japan, Kanagawa, Japan) were randomly divided into three groups, and their baseline nocifensive responses were measured. The mean latency was confirmed to be statically identical among the groups. The mice ($n = 9$) were then administered NC-4016 4 mg/kg or oxaliplatin 4 mg/kg on Days 0, 7 and 14 every 4 weeks over a period of 12 weeks (nine doses in total). Control mice were injected with 5% dextrose solution on the same schedule. After the nine administrations in total, the nocifensive responses in each group were measured again. Mechanical allodynia was assessed by measuring the latency of the paw withdrawal in response to noxious mechanical stimuli using a dynamic plantar esthesiometer (Ugo Basile, Varese, Italy). The mice were placed on a wire mesh floor in individual Plexiglas cages and allowed to acclimate for ~1 h, during which exploratory and grooming activity ended. A mechanical stimulus was applied to the plantar aspect of the hind paw using a metal filament with 2-mm diameter. The force was automatically increased at a fixed rate (0–5 g, 0.25 g/s) until the mouse withdrew its paw. The elicitations of the paw withdrawal responses were repeated four times at 10-s intervals. The paw withdrawal threshold (g) was calculated as the average of four measurements.

Statistical analysis

Data are expressed as mean ± SD. Repeated-measures ANOVA was used to evaluate the antitumor effects of the drugs and the changes in the body weight and cardiac function of each treatment group. Survival was assessed using the Kaplan–Meier method. Student's *t*-test was used to compare the nadir values of the blood cell counts. ANOVA with Tukey's multiple comparison was used to evaluate the changes in the nocifensive responses. The level of significance for all tests was set at $p < 0.05$. All statistical tests were two-sided. All analyses were conducted using SPSS, version 19.0 (SPSS, Chicago, IL).

Results

In vitro growth-inhibition assay

The IC_{50} values of NC-6300 and NC-4016 for the 44As3Luc cells were 55 ± 2.3 nM and 374 ± 19 nM, respectively. The IC_{50} values of epirubicin and oxaliplatin for the 44As3Luc cells were 15 ± 1.3 nM and 169 ± 13 nM, respectively. On the basis of these data, a molar ratio 1:10 was used for the NC-6300:NC-4016 and epirubicin:oxaliplatin combination studies.

Drug interactions between NC-6300 and NC-4016 (NCs) and between epirubicin and oxaliplatin (E/O)

Combination indices (CIs) of <1.0, 1.0 and >1.0 are indicative of synergistic, additive and antagonistic interactions between two agents, respectively. Marked synergism with a CI of 0.98–0.35 was observed between *Fa* 0.5 and 1.0 in both combination groups. The synergistic effect of NCs (Fig. 1*a*) was almost equivalent to that of E/O (Fig. 1*b*).

In vivo antitumor effect of single agents and combinations

Subcutaneous tumor.

The therapeutic effect of NC-6300 was significantly greater than that of epirubicin ($p = 0.047$). Similarly, the effect of NC-4016 was significantly greater than that of oxaliplatin ($p = 0.023$). The therapeutic effect of E/O was significantly

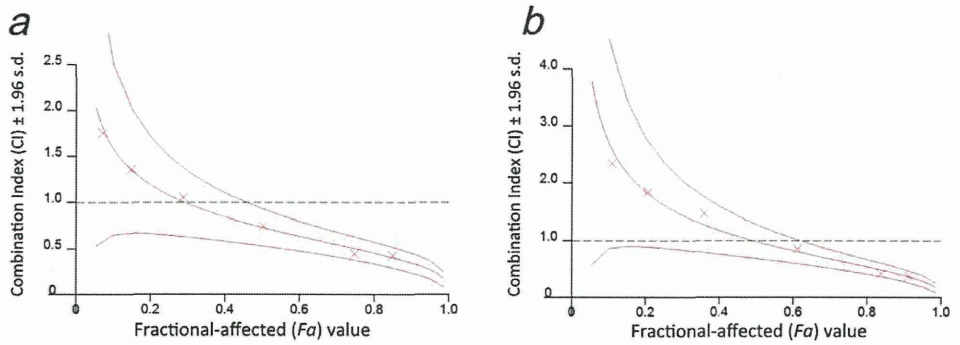

NC-6300 + NC-4016			
Fa	0.5	0.75	0.9
CI	0.732	0.503	0.349

Epirubicin + Oxaliplatin			
Fa	0.5	0.75	0.9
CI	0.981	0.613	0.391

Figure 1. CIs of the combined micelle (*a*) and free ACA regimens (*b*). CIs of <1.0, 1.0 and ≥1.0 are indicative of synergistic interactions, additive interactions and antagonism, respectively. NCs exhibited synergistic activity equivalent to E/O between *Fa* 0.5 and 1.0.

greater than that of epirubicin alone ($p = 0.001$) and oxaliplatin alone ($p = 0.002$). Likewise, the therapeutic effect of NCs was significantly greater than that of NC-6300 alone ($p < 0.001$) and NC-4016 alone ($p < 0.001$). Furthermore, the therapeutic effect of NCs was significantly greater than that of E/O ($p < 0.001$) (Fig. 2*a*).

There were slight and transient, but significant differences in the body weight loss between the single-agent and combined treatment groups (date not shown).

Orthotopic tumor

Comparison of the relative photon count until Day 28 in the 44As3Luc orthotopic model revealed that the antitumor effect of NCs was greater than that of E/O ($p = 0.016$). The antitumor effect of E/O was greater than that of control ($p < 0.001$) (Figs. 2*b* and 2*c*). On Day 28 after the initiation of each treatment, the localizations of the tumor in mice treated with NCs were restricted to the stomach of the primary site. On the other hand, widespread disseminations in the abdominal cavity were observed in the other two groups (Fig. 2*c*). The survival rate in the NCs group was also significantly superior to that in the E/O group ($p = 0.015$). Whereas there was no significant improvement between the E/O and control groups ($p = 0.173$) (Fig. 2*d*). There was no difference in the body weight loss or toxic death date between the two combined treatment groups (Fig. 2*e*).

Pharmacokinetic analysis

Next, we examined the concentration–time profiles of epirubicin and platinum in the plasma and various tissues of the mice after NCs and E/O administration. After E/O administration, the concentration of native epirubicin in the plasma and tumor decreased rapidly and the drug disappeared from both within 48 h. The C_{max} in the tumor was reached at 1 h after the injection. In contrast, after NCs administration, the highest intratumor concentration of free epirubicin released from NC-6300 was observed at 24 h, with the drug concentration remaining high for 3 days (Fig. 3*a*). NC-6300 was stable in the plasma and the amount of epirubicin released into the plasma was small (5%). The areas under the curve (AUC) ratios of free epirubicin released from NC-6300 to native epirubicin were 2.11, 3.78 and 4.99 in the tumor, plasma and liver, respectively. In contrast, the corresponding AUC ratio was only 0.27 in the heart. Furthermore, 42–53% epirubicin was released from NC-6300 in the normal tissues examined, while 81% was released in the tumor. The AUC of the epirubicin released in the liver was about fivefold greater than that of native epirubicin (Table 1).

Platinum derived from oxaliplatin cleared rapidly from the plasma and tumor after E/O administration (Fig. 3*b*). In contrast, platinum derived from NC-4016 after NCs administration gradually increased in the tumor and decreased in the plasma. The AUC ratios of platinum derived from NC-4016 to oxaliplatin were 3.69, 42.82 and 1.16 in the tumor, plasma and liver, respectively (Table 2). The platinum levels in the heart and small intestine were below the minimum limit of detection in both combination groups, and could not be evaluated.

Hematotoxicity, hepatotoxicity and nephrotoxicity of the combination therapies

The nadirs of the WBC and RBC counts in the E/O group were significantly lower than those in the NCs group ($p = 0.027$ and 0.007, respectively) (Fig. 4*a*). Slight and transient elevation of the hepatic transaminases was observed after the administration of NCs (Fig. 4*b*). No nephrotoxicity was observed in either group (Fig. 4*b*).

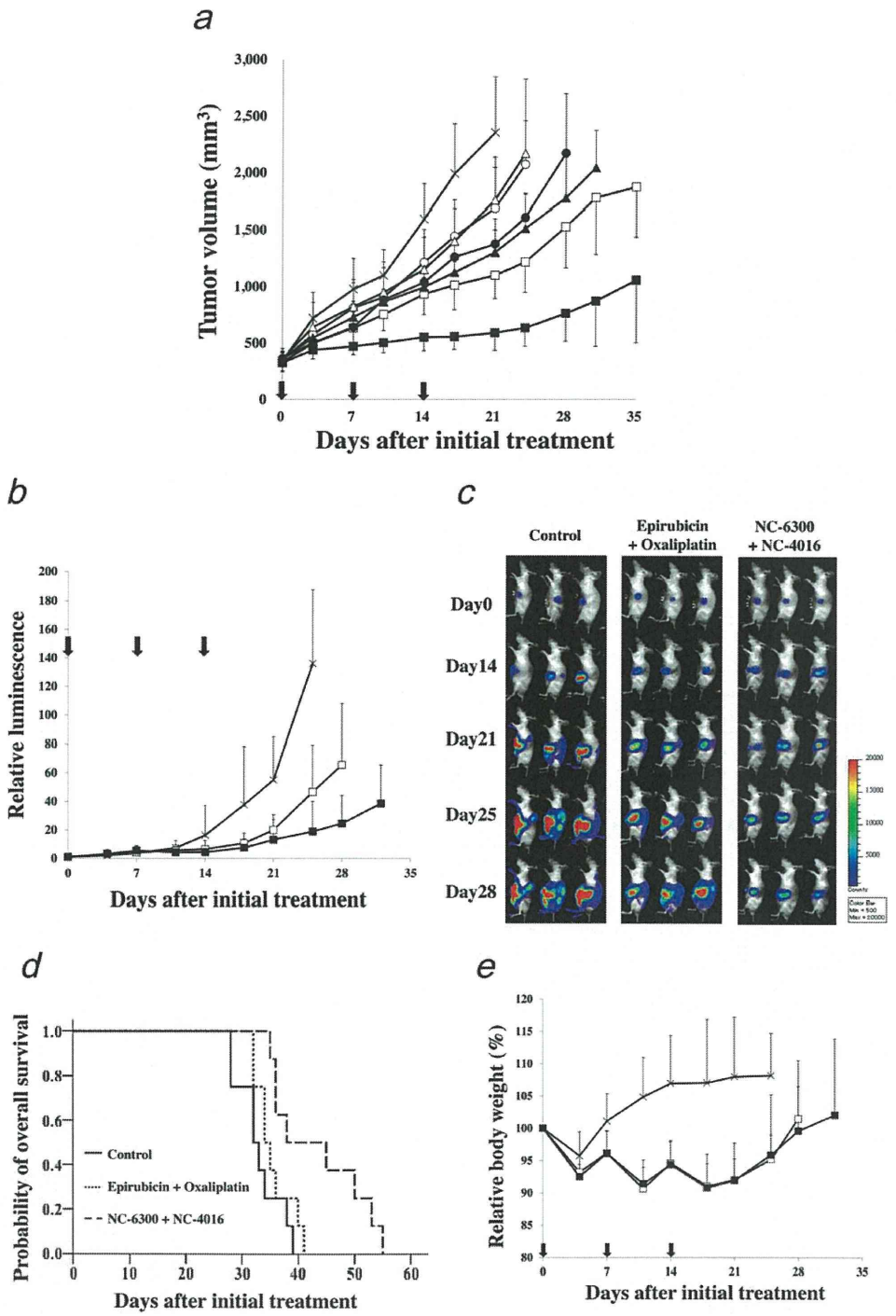

Figure 2. *In vivo* tumor growth inhibition assay. (*a*) Subcutaneous 44As3Luc xenograft models. The treatments were administered on Days 0, 7 and 14 after the tumor volume reached 300 mm^3 (Day 0) ($n = 5$). (×) Control, (○) epirubicin 8 mg/kg, (△) oxaliplatin 4 mg/kg, (□) epirubicin 8 mg/kg plus oxaliplatin 4 mg/kg, (●) NC-6300 8 mg/kg, (▲) NC-4016 4 mg/kg, (■) NC-6300 8 mg/kg plus NC-4016 4 mg/kg. *Points*, mean; *bars*, SD; *arrows*, drug injections. (*b–e*) Orthotopic 44As3Luc xenograft models. Seven days after the inoculation of 44As3Luc cells into the gastric wall (Day 0), the treatments were administered on Days 0, 7 and 14 ($n = 8$). (×) Control, (□) epirubicin 8 mg/kg plus oxaliplatin 4 mg/kg, (■) NC-6300 8 mg/kg plus NC-4016 4 mg/kg. (*b*,*c*) The antitumor activities using a photon-imaging system. *Points*, mean; *bars*, SD; *arrows*, drug injections. (*d*) Kaplan–Meier curves of mice bearing orthotopic 44As3Luc xenografts. (*e*) Changes in the relative body weight. *Points*, mean; *bars*, SD; *arrows*, drug injections.

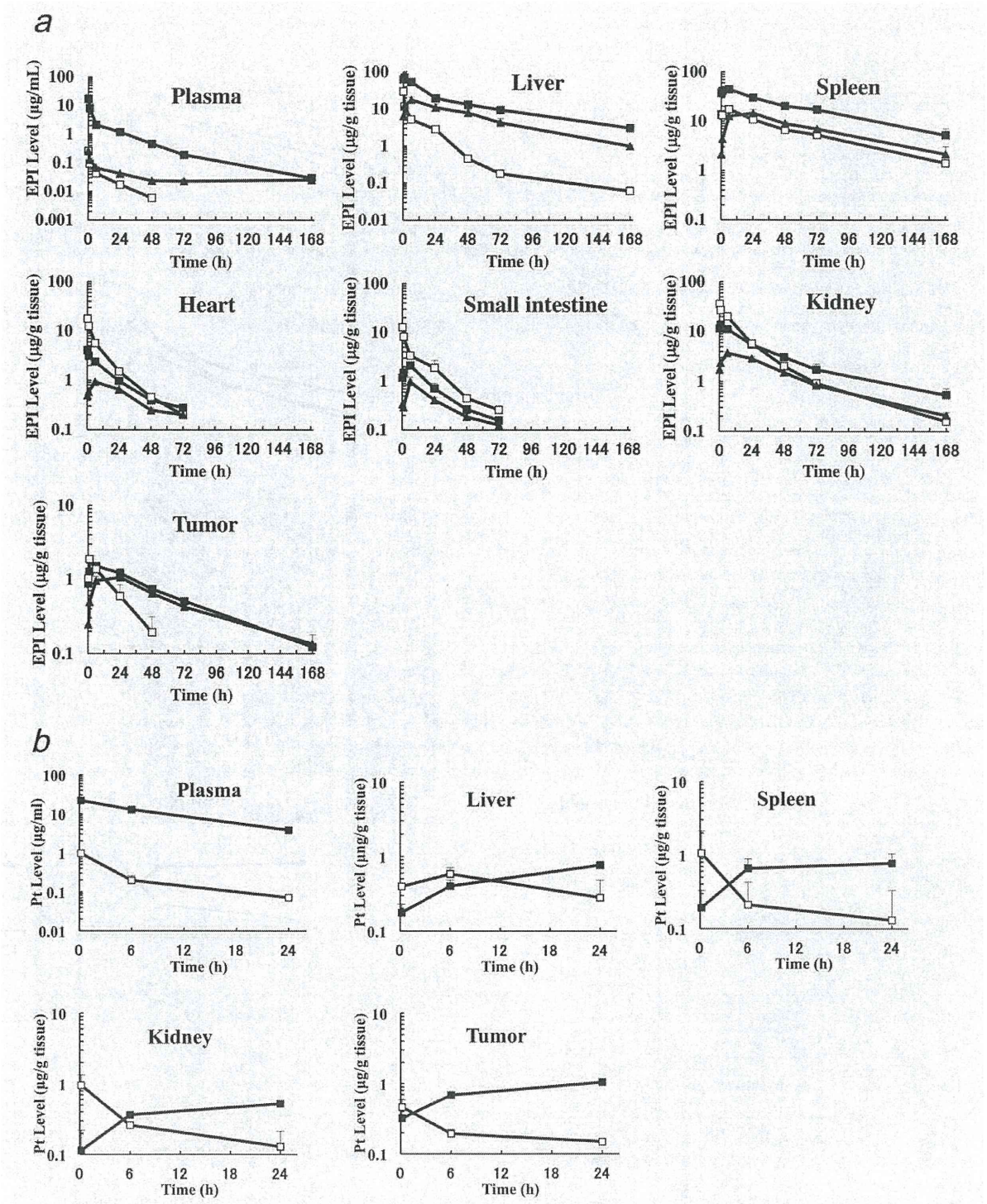

Figure 3. (*a*) Plasma and tissue concentration–time profiles of epirubicin (EPI) analyzed by HPLC after a single administration of NCs or E/O to mice bearing orthotopic 44As3Luc xenografts ($n = 3$). (□) Native epirubicin level from epirubicin 8 mg/kg plus oxaliplatin 4 mg/kg, (▲) released epirubicin level from NC-6300 8 mg/kg plus NC-4016 4 mg/kg, (■) total epirubicin level from NC-6300 8 mg/kg plus NC-4016 4 mg/kg. *Points*, mean; *bars*, SD. (*b*) Plasma and tissue concentration–time profiles of platinum (Pt) analyzed by ICP-MS after a single administration of NCs or E/O to mice bearing orthotopic 44As3Luc xenografts ($n = 3$). (□) Platinum level from epirubicin 8 mg/kg plus oxaliplatin 4 mg/kg, (■) platinum level from NC-6300 8 mg/kg plus NC-4016 4 mg/kg. *Points*, mean; *bars*, SD.

Table 1. AUC values of epirubicin in plasma and tissues after injection of NCs or E/O in mice bearing orthotopic 44As3Luc xenografts

	AUC (mg/g tissue or mL × h)				
	NC-6300				
	Released epirubicin	Total epirubicin	% Released	Native epirubicin	Released/native epirubicin AUC ratio
Plasma	5.3	104.9	5.0	1.4	3.78
Liver	954.7	2269.1	42.1	191.7	4.98
Spleen	1201.5	3048.0	39.4	1017.7	1.18
Kidney	206.7	491.8	42.0	559.7	0.37
Heart	44.2	84.8	52.1	164.8	0.27
Small intestine	32.7	61.5	53.2	134.2	0.24
Tumor	82.1	100.9	81.4	38.8	2.11

Table 2. AUC values of platinum in plasma and tissues after injection of NCs or E/O in mice bearing orthotopic 44As3Luc xenografts

	AUC (mg/g tissue or mL × h)		
	Platinum (Pt) from NC-4016	Platinum (Pt) from oxaliplatin	Pt (NC-4016)/Pt (oxaliplatin) AUC ratio
Plasma	253.03	5.91	42.82
Liver	12.30	10.64	1.16
Spleen	15.46	6.83	2.26
Kidney	9.39	7.08	1.33
Tumor	18.56	5.03	3.69

Cardiotoxicity and neurotoxicity

We assessed the cardiotoxicity induced by NC-6300 and epirubicin by transthoracic echocardiography. The EF was maintained within normal range in the mice treated with NC-6300 during and after the six administrations, and there was no difference in the EF between the NC-6300 treatment group and control group ($p = 0.076$). Whereas the mice treated with epirubicin exhibited a significantly lower EF than the NC-6300 treatment group ($p < 0.001$) and control group ($p < 0.001$) (Fig. 4*c*).

We next analyzed mechanical allodynia. After a total of nine administrations of each drug, the mice in the oxaliplatin treatment group exhibited a significantly lower mechanical threshold than the mice in the control group ($p < 0.001$) and NC-4016 treatment group ($p = 0.002$) (Fig. 4*d*). There was no statistically significant difference in the mechanical thresholds between the NC-4016 treatment group and control group ($p = 0.820$).

Discussion

Co-administration of anthracycline-based topoisomerase II inhibitors and platinum-based DNA-modifying agents is widely used in clinical practice.[13,30,31] The synergism between these two classes of drugs can be explained by the reciprocal interaction in which the inhibition of topoisomerase II partially hinders the efficient repair of DNA damaged by platinum alkylating agents.[32–34] In the present study, NCs exhibited synergistic activity equivalent to E/O. This suggests that the effective drug interaction between epirubicin and oxaliplatin was conserved *in vitro* in the combination of the corresponding micelles. Moreover, NCs exhibited significantly greater antitumor activity than E/O in the subcutaneous and orthotopic tumor models.

The pharmacokinetic analysis revealed that the AUCs of both epirubicin and platinum in the tumor tissue were greater following NCs administration than those following E/O administration, which clearly indicates that co-administration of two micellar formulations does not dampen their EPR effect in the tumors. NC-6300 and NC-4016 are very similar in terms of their mean micelle size, and the micellar surfaces are not modified with specific therapeutic components such as antibody, ligand or peptide. It remains unclear how the EPR effect might be influenced if micelles of differing sizes and/or surface-modified micelles were used in combination.

In regard to the toxicity evaluation, the degree of weight loss was almost the same between the NCs and E/O groups. Leukopenia and anemia were significantly milder in the NCs group than in the E/O group. Slight elevation of the hepatic transaminases was observed only in the NCs group. This hepatotoxicity has also been reported to be observed following administration of cisplatin-incorporating micelles.[35] Following systemic administration, micelles are likely to be distributed predominantly in the liver due to the developed mononuclear phagocytotic system of the liver and the rough filtration of relatively large molecules through the fenestrated sinusoidal endothelium. However, the hepatotoxicity is generally mild and transient, because most of the drug released from the micelles exists in the Kupffer cells rather than in the hepatocytes, as reported previously.[36] We also evaluated the cumulative toxicity induced by epirubicin and oxaliplatin. Patients treated successfully by long-term administration of these drugs sometimes need discontinuation of the effective drug due to its cumulative toxicity. Epirubicin and oxaliplatin have specific cumulative dose-limiting toxicities, namely, cardiotoxicity and peripheral neuropathy, respectively. Both toxicities were clearly and significantly lower in severity in the